

**164th Meeting of the Acoustical Society of America
Kansas City, Missouri
22 - 26 October 2012**

Session 3aNS: Noise

3aNS2. Full-scale rocket motor acoustic tests and comparisons with empirical source models

Michael M. James*, Alexandria R. Salton, Kent L. Gee, Tracianne B. Neilsen and Sally A. McNerny

*Corresponding author's address: Blue Ridge Research and Consulting, 29 N Market St, Suite 700, Asheville, NC 28801,
Michael.James@BlueRidgeResearch.com

Development of the next-generation space flight vehicles has prompted a renewed focus on rocket sound source characterization and near-field propagation modeling. Improved measurements of the noise near the rocket plume are critical for direct determination of the noise environment. They are also crucial in providing inputs to empirical models and in validating computational aeroacoustics models. NASA's SP-8072 acoustic load prediction model (1971) is a widely used method for predicting liftoff acoustics. The method implements two Distributed Source Methods (DSM-1 and DSM-2), which predict the loading as the sum of the radiated field from each source distributed along the plume. In this paper, measurements of a static horizontal firing of an Alliant Techsystem (ATK) Orion 50S XLG are analyzed with respect to the historical data that drive the SP-8072 prediction models. Comparisons include total sound power and sound power spectrum, and the distribution of the sound power and sound power spectrum along the length of the plume. Scalar pressure measurements yield reasonable agreement between the Orion-50S XLG data and both methods for undeflected plumes in the original SP-8072. However, development of these comparisons has prompted significant questions regarding the underlying physics of the two methods.

Published by the Acoustical Society of America through the American Institute of Physics

INTRODUCTION

The development of next-generation launch vehicles capable of travel beyond lower-Earth orbit has prompted investigations into improving accuracy of vibroacoustic load calculations. This requires improved source characterization and propagation models, particularly in the near field. As part of this process, improved measurements are essential, as they can help reveal source properties, serve as inputs to empirical models, and as benchmarks to computational fluid dynamics-based results.

An empirical, measurement-based methodology for predicting the noise content radiated by a rocket was developed for NASA in the early 1970's. This model is still in use and is generally referred to under its publication number NASA SP-8072, entitled "Acoustic loads generated by the propulsion system."¹ The calculation procedures outlined use source sound power distribution curves, in conjunction with directivity indices, to predict the radiated sound levels as a function of distance and angle. Because its models were developed using largely subscale measurements to produce its set of reference curves, recent efforts have been made to evaluate the SP-8072 model² using data collected on the four-segment reusable solid rocket motor (RSRM)^{3,4}. These updates have been used by Plotkin and Vu^{5,6} in launch pad noise prediction models.

The purpose of this paper is to examine how recently collected, near-field acoustic data from a 600 kN average thrust, solid rocket motor (the Orion-50S XLG) fit with the decades-old empirical source definition curves in SP-8072. In addition, results for the two different source sound power distributions are presented, along with a discussion of the underlying assumptions and implications for development of physically meaningful propagation models.

NASA SP-8072 OVERVIEW

Sound pressure spectra serve as the inputs for vibroacoustic models, and their accurate estimation is critical to the design of vehicles, payloads, and launch structures. Currently, the methodologies in SP-8072 are the only complete techniques for predicting the radiated sound levels from rocket motors.¹ The resulting sound pressure level predictions are based on three components: radiated power, frequency-dependent source locations, and directivity. The first two components are of concern in this paper. Directivity is treated in a companion paper.⁷

From SP-8072, the overall power, W_{OA} , is given as

$$W_{OA} = \eta N \left(\frac{T U_e}{2} \right), \quad (1)$$

where η is radiation efficiency, N is the number of nozzles, T is the thrust, and U_e is the exhaust velocity. Although more complete studies of the impact of N have since been carried out on noise generation from nozzle clusters (e.g. see Refs. 8 and 9), in this approximation multiple

nozzles simply scale the radiated power from one nozzle, with the total area altering the effective nozzle exhaust diameter, D_e .

There are two source allocation methods described in SP-8072, which have since been referred to as distributed source methods 1 and 2 (DSM-1 and DSM-2).² Although both methods involve dividing the plume up into multiple subsources, DSM-1 assumes that each frequency originates from a single, discrete subsource along the plume axis, with a sound power level for that frequency that collapses according to Strouhal number. On the other hand, DSM-2 first assumes a distribution for W_{OA} relative to the supersonic core length, x_t , and then assigns a sound power spectral shape, $W(f)$, for each subsource that varies jointly with position and frequency downstream. These two methods have the potential for defining a rocket plume very differently in terms of source content, while radiating the same overall power. Note that at the foundation of the SP-8072 source allocation is an assumption of incoherent radiation from subsources, though it is corrected by including far-field directivity indices as a function of frequency. In fairness, the monograph predates the body of knowledge regarding relatively large spatiotemporal correlation scales from large-scale turbulent structures in supersonic jets. (See Refs. [10-12]) Consequently, the continued evaluation of the source allocation models is important.

MEASUREMENT DESCRIPTION

Measurements were made during a ground-based midcourse defense (GMD) Stage 1 horizontal static test conducted at ATK's Promontory, Utah facility on 24 June 2010. This test occurred at ATK's T-6 test facility at approximately 11:06 a.m. Mountain Daylight Time (MDT). The GF058, or Orion 50S XLG, motor, has a 0.91-m (3.0-ft) diameter nozzle, and the solid fuel propellant was conditioned to a mean bulk temperature of 50° F, resulting in a burn time of 68 seconds. The motor's predicted maximum (vacuum) thrust occurs about 15 seconds after ignition and then remains fairly steady throughout the remainder of the test. The acoustic data used in this analysis was recorded during a 20 second time span in which the predicted thrust was steady at 622 kN (140,000 lbf).

On the two days prior to the static firing, measurement instrumentation was deployed in a field adjacent to the T-6 test facility, as shown in Figure 1. Measurement location distances are described in terms of nozzle diameters (D_e) with $1D_e$; angles are with respect to the motor exhaust direction. Three linear arrays, consisting of energy-based probes,^{4,13,14} pressure microphones, accelerometers, and meteorological sensors, were deployed.

The shear-layer array, indicated by the red dotted line in the rightmost photo of Figure 1, was offset by $10D_e$, 9.14 m, from the exhaust plume shear-layer boundary, which itself was estimated to be at a 20° angle to the motor centerline (including a 5° motor gimbal angle). This location permitted making acoustic measurements in the near-field environment while being far enough away from the plume to ensure that the instrumentation operated properly. Shear-layer measurement location distances are measured from the nozzle exit plane. Two additional radial

arrays were oriented at 60° and at 90° to the motor centerline, indicated in Figure 1 by the blue and purple dotted lines, respectively. Distances along the radial arrays were measured from the estimated peak source location, which is $15D_e$ downstream of the nozzle. Data were collected on a total of 47 channels at a sample rate of 204.8 kHz, using 24-bit National Instruments PXI-4462 cards. Additional details may be found in Ref. 13.

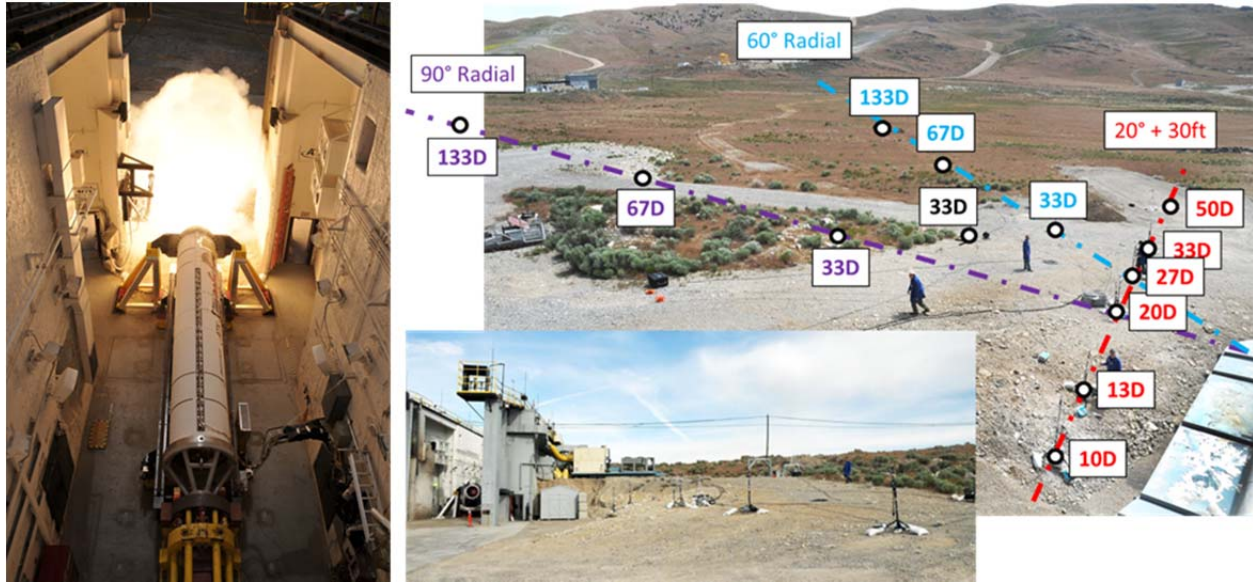


Figure 1. Photographs from the Orion-50S XLG measurement at ATK's Promontory, Utah facility on 24 June 2010.

MEASUREMENT RESULTS

The measurements along the shear layer array provide the opportunity to apply DSM-1 and DSM-2 to the Orion-50S XLG. The levels and spectra of the measurements are evaluated to provide inputs for the models. To use the shear layer array to estimate frequency-dependent sound power source distributions, an enveloping process was applied to the measured power spectra. First, the measured OASPL was reduced by 3 dB to estimate free-field conditions, as the rocket noise source was located above a hard ground plane radiating into half a volume as opposed to radiating into a free-field. Second, linear fits were applied to the measured narrowband spectrum (in decibels) at low and high frequencies and a Bézier curve fit was applied in the peak-frequency region. The resulting spectrum was scaled to preserve the OASPL. An example of this process is shown in Figure 2, with the narrowband spectrum at the left and the corresponding one-third octave spectrum on the right. As shown in Figure 3, the root-mean-square overall sound pressure levels (OASPL) along the shear layer array reach 154 dB re 20 μ Pa. The maximum region covers a relatively broad spatial source extent, considering these measurements were taken only $10D_e$ from the shear layer.

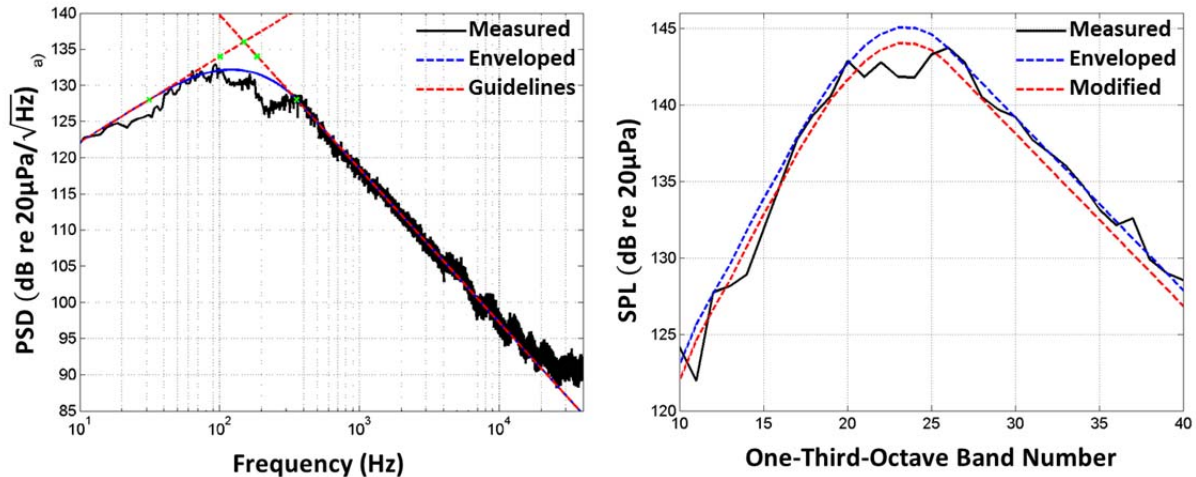


Figure 2. Example, using the Orion-50S XLG data, of the enveloping process used to obtain a modified spectrum, in which 3 dB is subtracted from the OASPL to account for the presence of ground interactions and curve fits were applied to smooth out ground interference effects in the peak region (left).

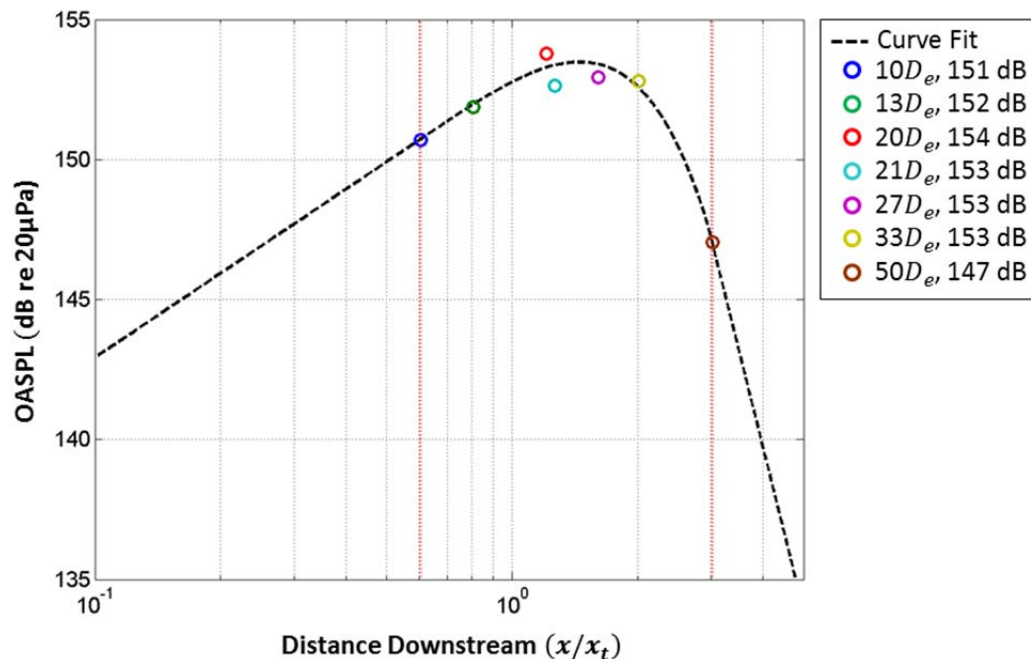


Figure 3. The root-mean-square overall sound pressure levels (OASPL) along the shear layer array (red dashed line in the rightmost photo in Figure 1) during the Orion-50S XLG measurement and a curve fit through the measurements to estimate the distribution of sound over a larger extent of the shear layer.

SOUND POWER ESTIMATION

To make comparisons between the Orion 50S XLG data and the empirical curves, an estimate of the overall sound power level (OAPWL) is needed. Although little detail is provided

in the SP-8072 monograph¹ as to how OAPWL was estimated for the various rockets and jets forming the database, it was found from arrays of individual pressure measurements. For the Orion-50S XLG measurement, we have used the pressure measurements along the shear-layer array and calculated a power level associated with each position by assuming axisymmetry and incorporating the surface area of a conical slice, A_i . This is written as

$$\text{OAPWL} = \sum_{i=1}^n [\text{OASPL}_i + 10 \log A_i], \quad (2)$$

and is illustrated in Figure 4. As with the spectral enveloping procedure, the OASPL at each position is reduced by 3 dB, before the OAPWL calculations, to estimate the radiation without the presence of the ground.

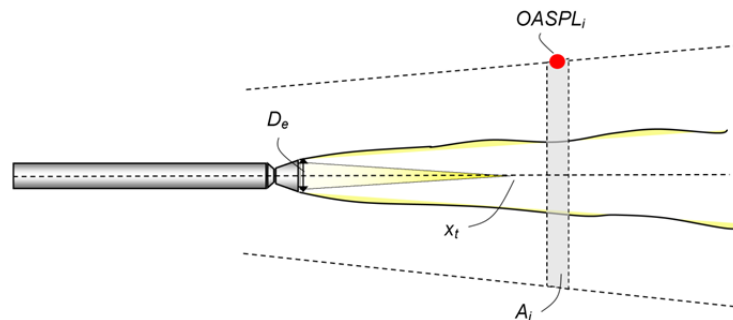


Figure 4. Schematic of how the OASPL measured along the shear layer multiplied by the area of a conical slice, centered of the nozzle exit and extending to the measurement point, is used to estimate the associated OAPWL.

Note that, because this approach relies on scalar pressure measurements, an important assumption is made. Sound power is correctly calculated as the surface integral of the intensity vector normal to the calculation surface. Without explicit directivity information at the source, it is assumed that squared pressure (or sound pressure level) is related directly to intensity at that location, which in turn assumes that the intensity vector is pointed normal to the conical surface. This approach results in an overestimate of OAPWL, given downstream directivity of the noise in the peak radiation region, such that the normal component of intensity is less than the total magnitude of the intensity vector, which is equal to the squared pressure.

An estimation of the OAPWL has been obtained based on the curve-fit distribution of OASPL shown in Figure 3 (after subtracting 3 dB). The calculation procedure in Eq. (2), for the Orion-50S XLG motor, results in an OAPWL estimate of 188 dB re 1 pW. This result can be checked for consistency against curves published in SP-8072¹ for different values of η (displayed in Figure 5) and from the work of Guest,¹⁵ where OAPWL is provided as a function of mechanical power, $TU_e/2$, in Eq. (1). Although the average vacuum thrust 622 kN (140,000 lbf) of the Orion-50S XLG is readily available, U_e is not. However, the nozzle exit velocity for the Orion-50S XLG is expected to be similar to that of the RSRM, given its similar propellant and scaled geometry, and consequently, a value^{2,3} of $U_e = 2454$ m/s was used. By applying the Orion-50S XLG estimated parameters to the SP-8072 model, the resulting predicted OAPWL

ranges between 179 and 189 dB re 1 pW. Assuming 0.5% efficiency, the predicted OAPWL for the Orion-50S XLG motor is 186 dB re pW, which is close to the Guest curve (shown as a blue line in Figure 5) that is based on a historical data that yields an estimate of 185 dB re 1 pW. Thus, the estimation procedure for OAPWL based on near-field scalar pressure data yields an estimate that is at least in accordance with prior estimation procedures and, as shown in Figure 5, very close to the previously estimated OAPWL from rockets with similar mechanical powers.

Before proceeding, the reader is reminded of uncertainties present in estimating the OAPWL both from measured data and from prior empirical curves. First, in estimating the OAPWL, the measured OASPL was first reduced by 3 dB to attempt to find the free-field radiated power. Second, the normal component of intensity was assumed to be equal to the total intensity magnitude. Finally, regarding the comparisons with prior data, neither U_e nor η are precisely known, which can result in a range of values for estimated OAPWL. However, the relative similarity in the estimates for OAPWL shown in Figure 5 suggest that these uncertainties are not prohibitive.

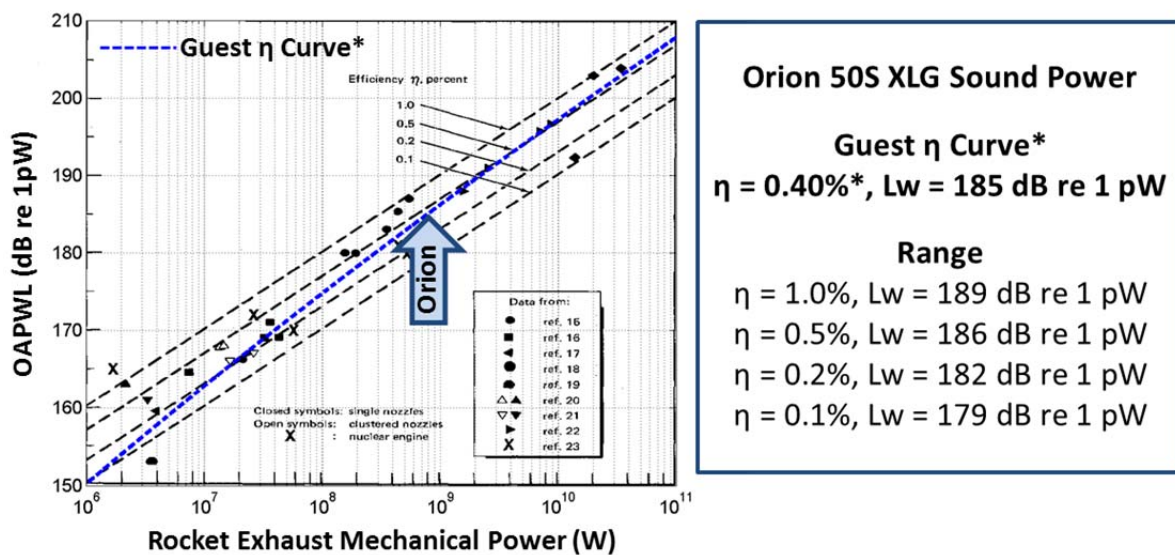


Figure 5. OAPWL as a function of rocket exhaust mechanical power as published in SP-8072,¹ with the prediction from the work of Guest¹⁵ shown as a blue dashed line and the estimated parameters for the Orion-50S XLG indicated by the blue arrow.

SOURCE ALLOCATION METHOD COMPARISON

The analysis thus far has resulted in an estimated OAPWL, with favorable comparison against prior empirical curves. These results do not, however, provide any information regarding how the power is distributed throughout the plume, either in terms of frequency or position. This latter information is essential in developing sound pressure level calculation procedures. Additional comparisons of the Orion-50S XLG data with the DSM-1 and DSM-2 source allocation models are now provided.

DSM-1

In the DSM-1 method, each subsource of the plume radiates only one frequency, with a relative power level that varies according to a spectral shape that is a function of Strouhal number, $St = fD_e/U_e$. The relative power level for the various downstream distances of the data used in SP-8072 resulted in the black curves shown in Figure 6. To find the apparent source axial locations as a function of frequency for the Orion-50S XLG measurements, the enveloped narrowband spectra were used to identify the location that had the maximum level for a given frequency. The Orion-50S XLG results are overlaid on the SP-8072 plots. Note that with the estimated U_e , $St \approx 0.1$ at 314 Hz. The resulting frequency distribution with position most closely follows that of the undeflected plume data from SP-8072, with the peak frequencies in the radiated spectrum (~ 50 - 200 Hz) originating in the 20 - $40D_e$ range. The relative OAPWL contribution closely follows the empirical curve derived from previous datasets, under the assumptions made in formulating it. Whether these results are accurate or simply yield a similar result as previous datasets that also forced estimation of required input parameters is unknown at the present. Still, the agreement with the normalized sound power spectrum is remarkable given that it matches the curve fit significantly better than any of the original data sets that were used to form it!

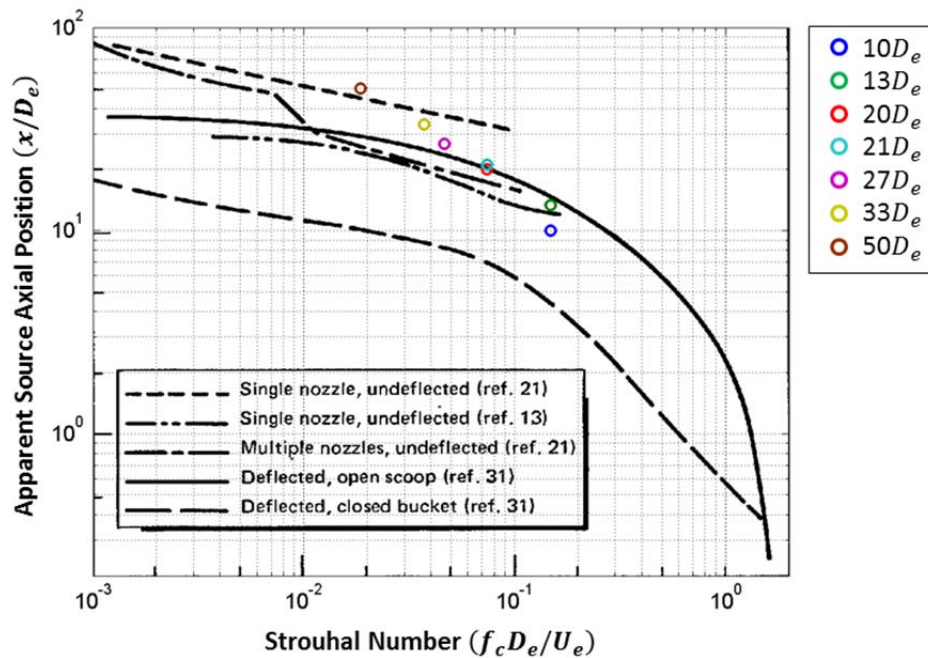


Figure 6. Empirical curves of apparent Axial Source Position (scaled by nozzle diameter) as a function of Strouhal number from Ref. 1 with the corresponding results for the Orion-50S XLG measurements shown as open circles.

DSM-2

In DSM- 2, the contribution to the OAPWL for each plume slice is determined relative to the supersonic core length. Then, each slice is assigned a spectrum according to an empirical spectral shape determined by a modified Strouhal number axis. The first step in this process is to examine how the normalized relative sound power spectrum from the Orion-50S XLG measurements compare to the data published in SP-8072.¹ This comparison, for measurements on the shear layer arrays, is shown in Figure 7, where the Orion-50S XLG normalized relative total sound power spectrum level is shown as a red line. The spectrum is a result of normalizing the total sound power spectrum over all seven measurement locations by the total power. The comparison shows very good agreement to the historical data supporting the continued practice of using the Strouhal number to collapse data sets from multiple engine nozzle dimensions. The spectrum is similar to those observed to the sideline and aft of military aircraft operating at high engine power.¹⁶

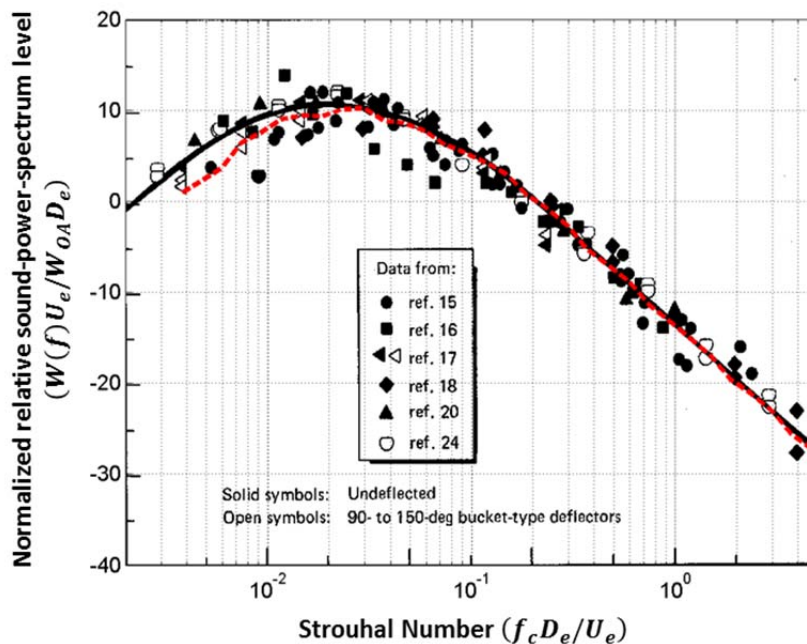


Figure 7. The normalized relative sound power spectrum from SP-8072¹ with the corresponding results for the Orion-50S XLG measurements shown as a red line. The red line represents the normalized relative total sound power spectrum level over the seven measurement positions.

The next step is to estimate the sound power per unit core length, in which the calculated core length, x_t , depends on U_e , D_e , and the speed of sound in the plume at the nozzle exit, c_e , taken to be 780 m/s. The measured points are again calculated by finding the intensity directly from the squared pressure and scaling by the conical slice area, as explained in Eq. (2). A curve fit and extrapolation from the measured points is performed to obtain a continuous function over axial position. The agreement in the shape of the OAPWL distribution both close to and far from the nozzle exit plane are ensured by prescribing the slope of the extrapolated curve in those

regions. The results for the Orion-50S XLG measurement agree well with the curve found in SP-8072,¹ as shown in Figure 8. Note that although others have proposed different methods for finding the supersonic core length,^{2,17} the shape of the distribution in Figure 8 would not vary from that shown here.

With the shape of the OAPWL distribution in hand, the frequency content of each slice needs to be assigned. The average normalized sound power spectrum for each measurement location, as a function of modified Strouhal number, is displayed in Figure 9. The dimensionless abscissa contains the product of frequency and distance, $f x$, which can be used in determining which spectral shape to apply at any given position, and a scaling factor related the ratio of the exhaust and ambient sound speeds and inversely related to the jet velocity. The average measured curves are compiled from the different spectra at all the measurement positions along the shear layer array. As a function of modified Strouhal number, the measured spectra mostly follow the same trend, which is slightly offset from the SP-8072 spectra. The main exception is the steeper high frequency slope for the $50D_e$ measurement. The similar offset in the peak radiation region and the frequency/distance on the high frequencies suggests a similar cause. Nevertheless, the normalized sound power spectra shapes are similar, though with slightly different roll-offs at large $f x$.

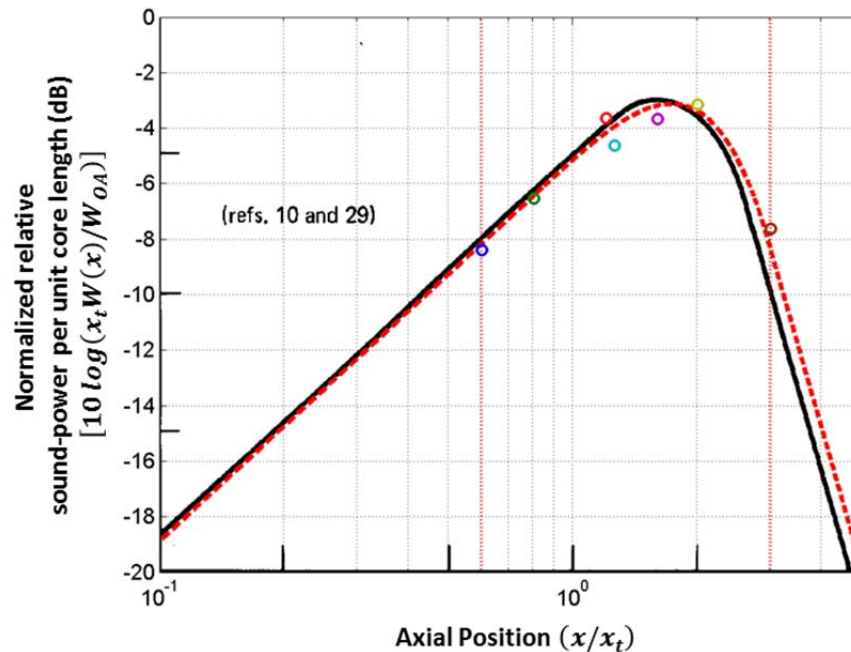


Figure 8. The normalized relative sound power level per unit core length from SP-8072¹ compared to the estimates for the Orion-50S XLG data (circles) and the extrapolated distribution (the red line). The colors of the circles correspond with measurement positions, as indicated in the legend of Figure 6.

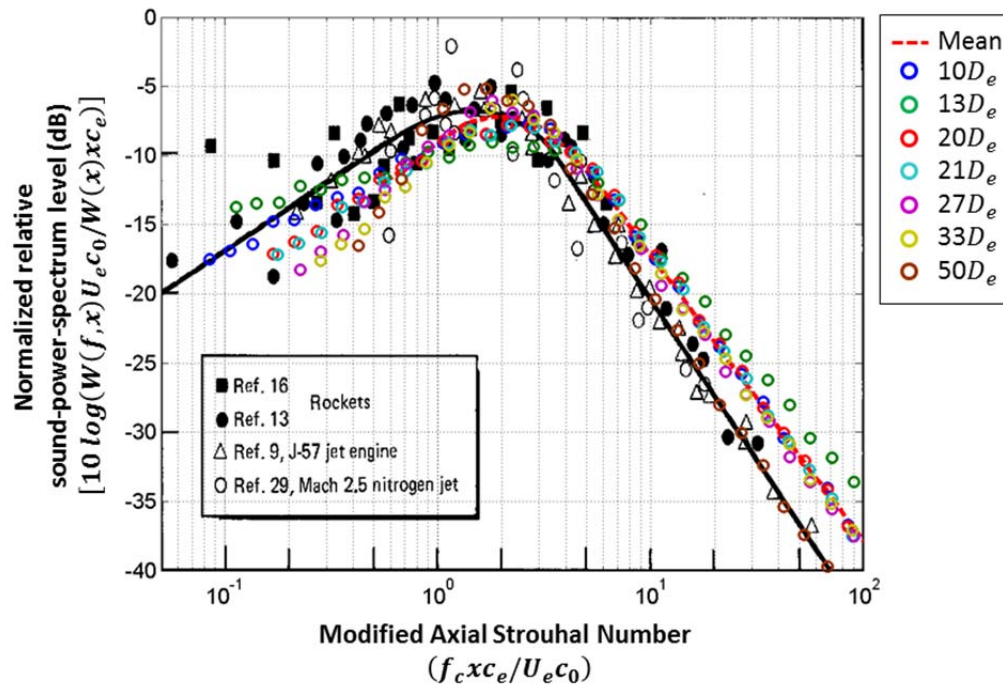


Figure 9. The average normalized sound power spectrum for each measurement location, as a function of modified Strouhal number from SP-8072¹ compared to the Orion-50S XLG results. The red line represents the energetic average of the spectra over the seven measurement positions.

CONCLUDING DISCUSSION

The distributed source methods 1 and 2 (DSM-1 and DSM-2) in NASA SP-8072¹ provide a way of allocating sound power as a function of frequency and axial position along the plume, as a precursor to predicting radiated pressure levels. With assumptions made at the outset, scalar pressure measurements yield reasonable agreement between the Orion-50S XLG data and both methods for undeflected plumes in the original SP-8072. However, development of these comparisons prompted significant questions regarding the underlying physics of the two methods. For example, DSM-1 uses curves directly from measured data to estimate source location but then makes the assumption that each subsurface only radiates a single frequency. On the other hand, DSM-2 allows for radiation of a full spectrum as a function of position but makes an assumption regarding the joint relationship of frequency and downstream position that does not collapse with the frequency/position curve in DSM-1, as shown in Figure 10. Thus, because DSM-2 prescribes a space-frequency relationship that does not appear to reflect properties of measured data, its ability to accurately predict the apparent source axial position on a frequency basis is questionable.

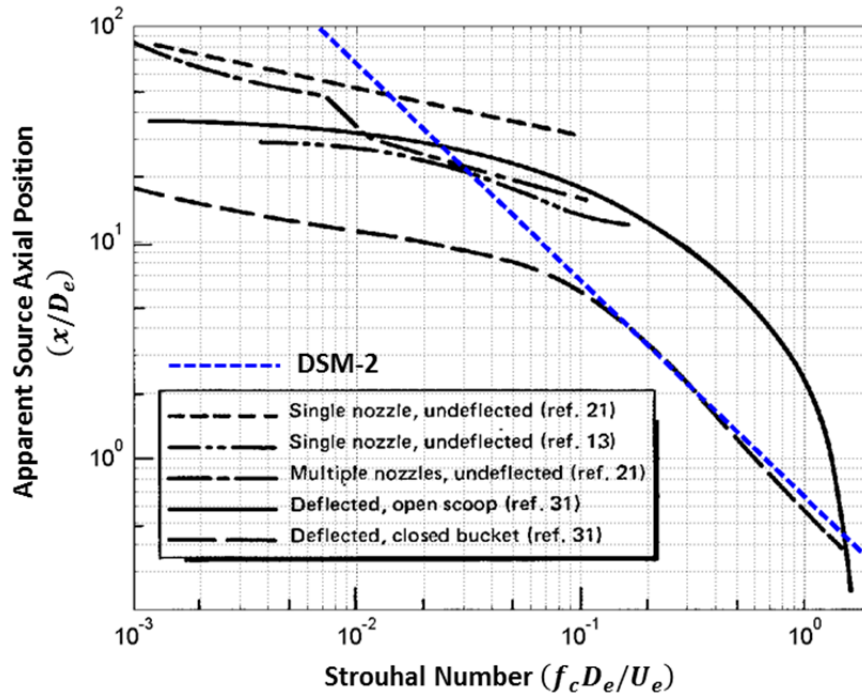


Figure 10. Apparent Source axial position obtained using DSM-2 (blue line) does not resemble the curves published in SP-8072¹ or those obtained with DSM-1 shown in Figure 6.

Recall that these methods represent the source allocation portion of a radiation model. Collapse of equivalent source distributions with the data does not confirm these methods will predict the sound pressure level radiation. Furthermore, even if the physics bears out the rationale for either or both of the DSM-1 and 2 methods, distribution shapes and frequency content are not enough to yield accurate estimates of the radiated sound pressure level. Accurate estimates of the overall radiated power are essential. Vector intensity measurements, such as those shown by Gee et al.^{4,14,18} and James and Gee¹³ should provide a path forward to more accurately use near-field measurements to directly obtain estimates of radiated power.

ACKNOWLEDGMENTS

This work has been supported by a Small Business Innovation Research (SBIR) program sponsored by NASA Stennis Space Center. The authors wish to thank Dr. William W. St. Cyr of NASA Stennis Space Center, and Alliant Techsystems Inc. for supporting the Blue Ridge Research and Consulting, LLC and Brigham Young University team.

¹ K.M. Eldred, "Acoustic loads generated by the propulsion system," NASA SP-8072, (1971).

² J. Haynes and R. Kenny, "Modifications to the NASA SP-8072 Distributed Source Method II for Ares I lift-off environment predictions", AIAA paper 2009-3160, May 2009.

³ R. J. Kenny, C. Hobbs, K. Plotkin, and D. Pilkey, "Measurement and characterization of Space Shuttle solid rocket motor plume acoustics," AIAA paper 2009-3161, May 2009.

-
- ⁴ K. L. Gee, J. H. Giraud, J. D. Blotter, and S. D. Sommerfeldt, "Energy-based acoustical measurements of rocket noise," AIAA paper 2009-3165, May 2009.
- ⁵ K. J. Plotkin and B. T. Vu, "Further development of a launch pad noise prediction model," *J. Acoust. Soc. Am.* **130**, 2510 (2011).
- ⁶ K. J. Plotkin and B. T. Vu, "Extension of a launch pad noise prediction model to multiple engines and directional receivers," *J. Acoust. Soc. Am.* **132**, 1991 (2012).
- ⁷ M. M. James, A. Salton, K. L. Gee, T. B. Neilsen, S. A. McInerny, R. J. Kenny, "Modification of directivity curves for a rocket noise model," submitted to *Proc. Mtgs. Acoust.*
- ⁸ M. Kandula, "Nearfield acoustics of clustered rocket engines," *J. Sound Vib.*, 309, 852-857 (2008).
- ⁹ I. S. Coltrin, J. D. Blotter, R. D. Maynes, and K. L. Gee, "Shock-cell structures and corresponding sound pressure levels emitted from closely spaced supersonic jet arrays," *Appl. Acoust.* **74**, 1519-1526 (2013).
- ¹⁰ C. K. W. Tam, K. Viswanathan, K. K. Ahuja and J. Panda, "The sources of jet noise: experimental evidence," *J. Fluid Mech.* **615**, 253-292 (2008).
- ¹¹ K. Viswanathan, J. R. Underbrink and L. Brusniak, "Space-Time Correlation Measurements in Near Fields of Jets," *AIAA J.* **49**, 1577-1599 (2011).
- ¹² B. M. Harker, K. L. Gee, T. B. Neilsen, A. T. Wall, S. A. McInerny, and M. M. James, "On autocorrelation analysis of jet noise," *J. Acoust. Soc. Am.* **133**, EL458 – EL464 (2013).
- ¹³ M. M. James and K. L. Gee, "Advanced acoustic measurement system for rocket noise source characterization," *Proc. Internoise 2012*, paper in12_1127 (2012).
- ¹⁴ K. L. Gee, J. H. Giraud, J. D. Blotter, and S. D. Sommerfeldt, "Near-field acoustic intensity measurements of a small solid rocket motor," *J. Acoust. Soc. Am.* **128**, EL69-EL74 (2010).
- ¹⁵ Guest, S. H., "Acoustic Efficiency Trends for High Thrust Boosters," *NASA TN D-1999*, July 1964, MSFC.
- ¹⁶ T. B. Neilsen, K. L. Gee, A. T. Wall, and M. M. James, "Similarity spectra analysis of high-performance jet aircraft noise," *J. Acoust. Soc. Am.* **133**, 2116 – 2125 (2013).
- ¹⁷ J. Varnier, "Experimental study and simulation of rocket engine freejet noise," *AIAA J.* 39, 1851-1859 (2001).
- ¹⁸ T. A. Stout, K. L. Gee, T. B. Neilsen, A. T. Wall, D. W. Krueger, and M. M. James, "Preliminary Analysis of Acoustic Intensity in a Military Jet Noise Field," *Proc. Mtgs. Acoust.* **19**, 040074 (2013).